

A Novel Approach to Foam Cement

Allen Kelley, Cornell Stanciu, Kristina Fontenot and Jorge Fernandez, Sasol Performance Chemicals

Copyright 20209, AADE

This paper was prepared for presentation at the 2020 AADE Fluids Technical Conference and Exhibition held at the Marriott Marquis, Houston, Texas, April 14-15, 2020. This conference is sponsored by the American Association of Drilling Engineers. The information presented in this paper does not reflect any position, claim or endorsement made or implied by the American Association of Drilling Engineers, their officers or members. Questions concerning the content of this paper should be directed to the individual(s) listed as author(s) of this work.

Abstract

The complexities of drilling in shale formations has fueled the drive for lightweight economical cement slurries. Many of the wells in West Texas have multiple weak or brittle zones within a few thousand feet, requiring low density specialty cement systems to ensure the long-term health of the well. This positions foam cement to become an industry standard when cementing in complex formations. In this paper a range of non-ionic ethoxylates are used to enhance anionic surfactant-based cement foam packages, for the US market. Results are compared to two currently available commercial cement foamers, as well as an oilfield cement foamer.

By reducing the cement foam quality to 50% it is shown that cement foam packages consisting of 100% anionic surfactants will not always produce the most stable foam and that non-ionic ethoxylates can enhance foam stability and increase the cement bond to the formation. Novel surfactant packages are demonstrated to make a wide range of stable foam qualities (>50%) over a wide range of temperatures (70-150 °F). To give an enhanced picture of how the novel based cement foamer interacts inside of the cement matrix, the density and microstructural bubble sizes in the samples are compared at 4 different heights.

The non-ionic ethoxylates were not able to create a stable 50% foam quality cement on their own. However, they were able to dramatically reduce the amount of anionic surfactant needed to produce the 50% foam quality. There are also clear and predictable trends in the effectiveness of the novel ethoxylate vs. the concentration added, allowing for a surfactant package to be built and optimized with minimal testing. The concentration of anionic surfactant used to create the foam cement is important because the anionic surfactants are notably more expensive than their non-ionic counterparts.

The contents of this paper are meant to help engineers design and optimize a surfactant package for a foam cement job. The performances of various anionic surfactants are compared to blends of non-ionic and anionic surfactants. The line shapes of three novel ethoxylates are presented allowing extrapolation to generate theoretical loadings for all liquid non-ionic ethoxylates tested.

Introduction

The application of foam cement has been widely used in the oil & gas industry, especially in cases where densities lower than that of water are required (McElfresh and Boncan 1982). There are several benefits to using foam cements. Foam cement exhibits a more elastic response to mechanical strain than the base slurry, showing a lower Young's Modulus (Iverson, Darbe and McMechan 2008). Reducing Young's Modulus enhances the foam cements ability to flex under stress, reducing the probability the cement will de-bond from the wellbore or formation, preventing the formation of micro annuli and fluid migration between zones (Goodwin and Crook 1992). Foam cement is especially good at cementing casing in weak or brittle formations. The low-density high strength cement reinforces the fragile formation and prevents cement fallback, while minimizing formation damage (Peskunowicz and Bour 1987).

Foam cements mechanical and physical properties vary with density, however, the chemical properties of the base slurry are unaffected. This allows the properties of foamed cement to be divided into two groups. The first group arises from the design of the base slurry. The design of the base slurry, primarily affects the chemical properties of the foam cement (fluid loss, thickening time and resistance to wear). The second group contains everything that effects the bubble size distribution (BSD) (surfactant, foam quality, foam stability, pressure and mixing procedure). This second group directly affects the mechanical properties of the foam cement (rheology, compressive strength and Young's Modulus). All the properties are important to the final cement design, highlighting the importance of using a well-designed base slurry and a good surfactant package.

Foam cement is created by adding a surfactant package to the base slurry, then impregnating the slurry with nitrogen or air bubbles. The bubbles must form a uniform mixture and remain stable, meaning that the gas bubbles should not coalesce. In order to create foam, a surfactant must be sufficiently surface-active to stabilize a newly formed air/water interface and reduce the surface tension of the air/water interface. The stabilized bubble must also have elasticity, meaning that once formed it can withstand being perturbed by external forces without expanding. This means that surfactants with high concentrations of monomers dissolved in the bulk phase will not form stable foams. This is due to the monomers

ability to stabilize the perturbed bubble before the surfactant film can spread over the surface restoring the bubble to its original size. A surfactant with good foam-ability is highly surface active, with few monomers, a low critical micelle concentration, the micelles must diffuse fast enough to the water/air interface to stabilize the newly created bubbles, but not so fast as to damage the elasticity.

Once the slurry bubbles are entrained into a foam, the foam is subject to 4 major forces. These forces determine the stability of the foam. They are gravitational, pressure differences between lamellae and plateau borders, pressure differences between gas bubbles and repulsion between electrical double layers. The gravitational force causes drainage inside the foam, pulling the liquid through the plateau borders and thinning the lamellae as it flows back to the bulk. The pressure differences between lamellae and plateau borders also causes the thinning of the lamellae. As the drainage occurs the plateau borders and lamellae thin, forming a low-pressure region as the curvature of the surface in the plateau borders changes, further thinning the lamellae as liquid is pulled from the lamellae regions. The entrained bubbles that comprise the foam can have different internal pressures. This gives rise to bubbles of different sizes, where larger bubbles have lower internal pressures than smaller bubbles. The smaller bubbles can transfer gas to the larger bubbles through a process known as Ostwald ripening. In theory a foam can be destroyed through this process without any coalescence occurring. The electrical double layer is formed from the head group of the anionic/cationic surfactant interacting with the interface. For anionic/cationic surfactants the charged head groups in the thin film can be modeled like a Gauss surface, generating a Coulomb repulsion as the lamellae are thinned and the two parallel films are brought in close proximity. The repulsive force can stop the thinning of the lamellae, stop drainage and stabilize the foam. Non-ionic surfactants have also been shown to form small surface potentials between thin films as they are brought into close proximity (Prud'homme and Khan 1996).

This paper will look at creating surfactant packages for foam cement using cheaper short chain non-traditional surfactants. The surfactants normally used in cement foamers are 12-16 carbon chain ethoxylates, which are traditionally sold into the home and personal care markets. The utilization of the shorter chain non-traditional surfactants will allow companies to cut cost while maintaining performance in many situations.

Experimental

There are no specific API standards for testing foam-ability of foam cement surfactant packages. This property is very important because it dictates the concentration of surfactant that must be used to create a specific quantity of foam cement. With the lack of universal standards companies have developed their own standards and methods for evaluating this property. Foam-stability testing is described by API 10B-4, this gives a general outline of how to determine the overall stability of the foam cement blend. It doesn't determine the cause nor quantify the

extent of the foam degradation within the system. By quantifying foam-ability and foam-stability parameters, a systematic study can be used to find low cost-efficient alternatives to commonly used surfactants. The authors use the Bikerman method to find the foam-ability and the Ross-Miles method to find foam-stability of surfactant blends in aqueous solutions. It must be noted that an aqueous system and a cement system are vastly different, therefore the results obtained in aqueous systems don't fully represent the surfactant-system interactions that occur in cement systems. For this reason, the authors introduce an innovative approach to determine foam-ability in cement systems and use a two-step evaluation to find foam-stability. The two-step method relies on the API 10B-4 stability testing and an analysis of the BSD left behind after the cement is cured.

The Bikerman method was developed to find the foam-ability of surfactants in aqueous systems. In this method a controlled stream of air is forced through a frit into a set amount of surfactant solution. The controlled rate of air into the system balances foam generation against foam degradation. The foam-ability of the system can then be found based upon surfactant concentration. By keeping the surfactant concentration low and measuring the time and hence the rate for a foam to reach a specific height, the foam-ability can be found. It must be noted that the in the experiments all surfactants are compared using $\frac{\text{ml surfactant}}{\text{L}}$ because surfactants are sold by volume not moles, a true comparison would require the use of $\frac{\text{M surfactant}}{\text{L}}$. The foam-ability is found using the KRUSS DFA100 by adding 50 ml of the $\frac{1}{6}$ concentration solutions given in Figure 1 to the column and bubbling air through the frit at $200 \frac{\text{ml}}{\text{min}}$. The foam rises in the column until a maximum height is reached, the rate of foam generation can then be calculated.

The Bikerman method works well in aqueous solutions, however there isn't any commercially available equipment to utilize this method for cement systems. The foam-ability of the cement mixture is measured by finding the amount of surfactant required to create a 50% foam quality cement using API 10B-4 mixing standards. The cement and surfactant package are poured into a 5 bladed blender cup at room temperature and mixed on high shear for 15 seconds. The resulting foam density is calculated using a weighed 100 ml graduated cylinder. The foam-ability of the cement paste is found by adjusting the surfactant concentration and repeating until a repeatable 50%

$\pm 1.5\%$ foam quality is achieved, Figure 1.

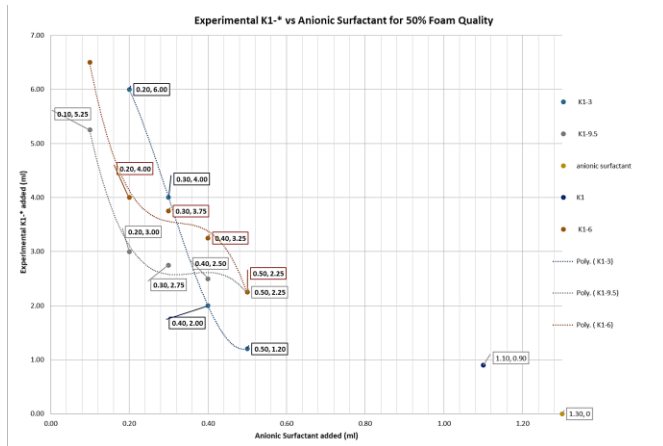


Figure 1: Foam-ability of the surfactant blends in cement at 70°F. Each blend is standardized by the minimum amount of surfactant required to produce a 50% foam quality.

The Ross-Miles method is used to find the foam stability in aqueous solutions. In this method the foam stability is measured by calculating the rate of collapse in the aqueous foam. Measurements are taken every $\frac{1}{2}$ s with the rate being calculated at 5 and 10 minutes using the KRUSS DFA100. 60 ml of solution with surfactant concentration equal to thoughts described in Figure 1 to create a 50% foam quality are added to the column. Air is injected through the frit at a rate of $600 \frac{\text{ml}}{\text{min}}$, once the specified height is reached the foam height is recorded every $\frac{1}{2}$ s. The rate of collapse is calculated by finding the slope of the foam-height (decay) vs time graph.

The foam stability of the cement paste is measured using stability testing described in API 10B-4 and analyzing the bubble size distribution BSD. For the room temperature stability test the cement paste and surfactant package are blended in a 5 bladed blender cup, giving a final quality of 50%. The foam is placed into a cement settling tube and allowed to cure for 7 days. Once cured the cores are cut into 4 pieces (Top, Middle Top (MT), Middle Bottom (MB) & Bottom (Bot)), the top of each piece is colored black by a sharpie and the bubble voids are filled with silica flour. Pictures of these cores are analyzed by ImageJ for BSD (Schneider, Rasband and Eliceiri 2012). The images are converted into grayscale and thresholded by 50%. The image is next watershed and the bubbles are counted with the area of each bubble being calculated. For testing above room temperature, the cement paste is conditioned up to testing temperature for 30 minutes using an OFITE model 60 atmospheric consistometer. The 5 bladed blender cup and settling tubes are heated to temperature prior to mixing. This keeps the slurry close to the desired temperature throughout the foaming process. Once mixed the slurry is quickly poured into the settling tube and placed into the oven for curing at desired temperature for 7 days. It must be noted that this is all done under atmospheric pressure and that small

deviations in temperature during this process can greatly affect bubble size.

The cement slurry used is 15 lb/gal and created using 100% TXI type I/II Portland cement. The slurry was mixed for 15 s on low shear and 35 s on high shear using an OFITE model 20 constant speed blender with a 1-liter cement blender cup following API 10B-4 mixing standards. After mixing, the initial density of the cement blend is calculated using a weighed 100 ml graduated cylinder. The thickening time is estimated by pouring the base cement into a plastic cup and allowing it to set at experimental temperature. The requirements imposed upon the design, were that the cement had to be flowable after 6 hours and fully set in 24 hours for elevated temperature runs. At room temperature the cement just needed to set. API 10B-4 atmospheric settling tests were performed at a 90° angle and only at room temperature. The viscosity of the slurry was recorded using a Grace model M3600 viscometer.

Results

Foam cement surfactant packages are often designed in house at service companies. These designs have been used for decades with proven results. With the current challenging macroeconomic environment in the upstream oil and gas market, a movement towards competitively priced products with comparable performance is allowing formulators to become creative with the designs that are being introduced into the market. This has led to a very fast shift in the chemicals that are being utilized within the oil and gas market. Pressure to maintain profitable operations are forcing companies to reevaluate their chemical portfolios, including surfactants for foam cement.

The base cement blend for room temperature testing is composed of 100% TXI type I/II Portland cement with 0.50% NaCitrate. The retarder loading for this blend is purposefully high, allowing a long period of time for the foam to collapse. The cup thickening time test for this blend showed that it remained fluid for 24 to 36 hours and fully sets in 72 hours, giving the foam ample time for coalescence or Ostwald ripening to occur. The API settling test showed 6 ml of free water and the rheologies were workable as shown in Figure 2. Figure 2 shows that the cement rheology is greatly affected by temperature and retarder loading, however the change between the two blends is minimal and the reduction in viscosity due to the increased temperature is partly offset by the reduction in retarder from the base blend. This affects the gel strengths as well with the $\frac{10\text{s}}{10\text{min}}$ gel strengths for the 70°F slurry being $\frac{13.4\text{deg}}{17.8\text{deg}}$ and the gel strengths for the 151°F slurry being $\frac{9.6\text{deg}}{11.4\text{deg}}$. Highlighting that we expect there to be more stability issues at the elevated temperatures due partly to the cement blend. The increase in kinetic energy of the system along with the reduction in gel strength will leading to enhanced coalescence. It must be noted that as the temperature is increased only the retarder loading is changed.

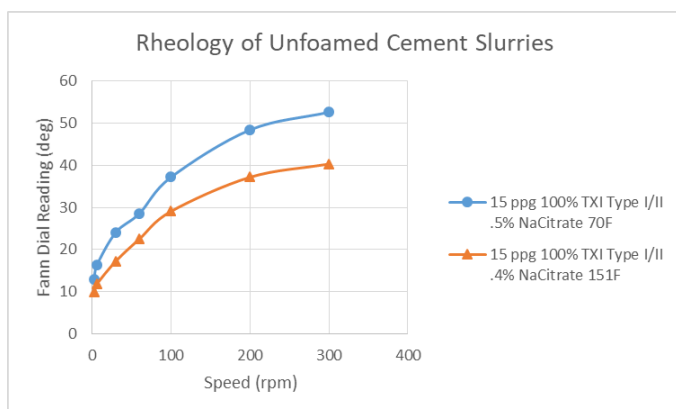
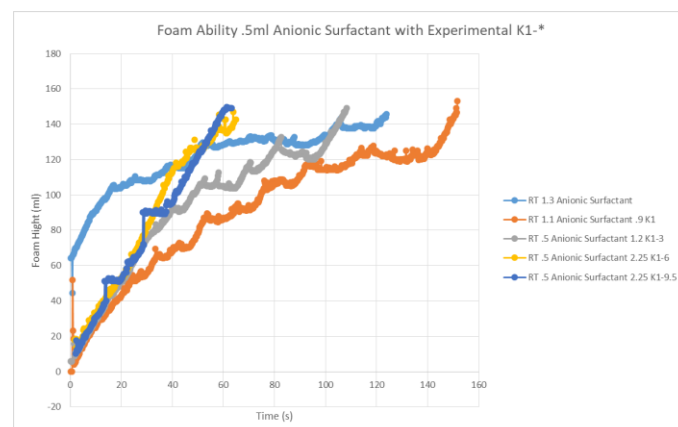


Figure 2: Rheology of the unfoamed cement slurries without surfactant used for testing at room temperature (70°F) and 151°F.

The foam-ability of the surfactant packages is in practice a measure of the efficiency of the foamer, relating how much surfactant must be used to create a specific amount of foam or cement quality. The foam ability of the surfactant packages in the 70°F base cement slurry is shown in Figure 1. This plot takes a cubic form and shows two distinct regions, with distinctly different chemistries. The first region is between .1ml(.0015gps) and .2ml(.003gps) of the anionic surfactant and .4ml(.006gps) for the Experimental K1-3. In this region the slope of the graph is very steep, and the nonionic surfactant is the primary foamer. It is easily seen by the increase in nonionic surfactant required to produce the desired foam quality, that the anionic surfactant has the highest foam-ability in the cement system and is therefore the most efficient foamer. It must also be noted that none of the nonionic surfactants used were able to create the desired foam quality, even using 10ml(.15gps) loadings on their own. The second region is between .2ml(.003gps) and .5ml(.008gps) of anionic surfactant, in this region the slope dramatically decreases, the nonionic surfactant is still the primary foamer and the anionic surfactant is increasing the foam-stability leading to a higher foam-ability. Experimental K1 normally acts as a defoamer, it increases the solubility of the hydrophobe in solution and thins the surfactant at the lamellae increasing coalescence. It is surprising to see that at low concentrations it dramatically increases the foam-ability of the cement system. The interaction with the hydrophobe reduces the coulombic repulsion felt by the head groups and increases the critical packing parameter (CPP) at the interface stabilizing the foam. Figure 1 shows that the Experimental K1-9.5 has the highest foam-ability for nonionic surfactants in the cement system up to 4ml(.006gps) of anionic surfactant and that between 3 and 4ml of anionic surfactant with Experimental K1-3 has the highest foam-ability.

The difference between the foam-ability of surfactant packages in aqueous and cement systems is of profound importance in this discussion. With the lack of dedicated cement equipment to discern the foam-ability most companies rely on aqueous testing. The foam-ability of the blends required to produce the 50% foam quality in cement systems needs to be

tested using standard industry techniques so that they can be reliably reproducible. The Bikerman method is used to do this in aqueous solutions. The surfactant concentrations are diluted to allow the surface activity and rate of diffusion to influence the foam-ability, Figure 3 shows these results. In Figure 3 the blue line represents the foam-ability of pure anionic surfactant which is used as the baseline with which we will describe the chemistry observed. The orange line represents the blend of anionic surfactant and Experimental K1. This combination is interesting because as the chemistry of Experimental K1 is typically better suited as a defoamer as shown in the aqueous test. In Figure 1 small concentrations of Experimental K1 increased the foam-ability in the cement system, showing that the Experimental K1 surfactant interaction is different in both systems. The plots in Figure 3 show that the Experimental K1-6 blends almost uniformly have the highest foam-ability, at room temperature. The .5ml anionic surfactant-1.2ml Experimental K1-3 blend shows a dramatic reduction in foam-ability when compared to the other plots, this is expected in aqueous solution because of the low concentration of Experimental K1-3. In this system, Experimental K1-3 is reducing the coulomb repulsion between the anionic surfactant increasing the CPP. Therefore, the line shape looks like the anionic surfactant with a slightly higher foam-ability. When the Experimental K1-3 concentration is increased from .5ml anionic surfactant-1.2ml Experimental K1-3 to .4ml anionic surfactant-2ml Experimental K1-3 the Experimental K1-3 becomes the main foamer and the line shape becomes uniform with the other plots. The foam-ability in aqueous solution of the Experimental K1-3 is decreasing with increasing concentration of anionic surfactant while the opposite is true in the cement system, while the Experimental K1-9.5 generally has the lowest foam-ability of the nonionic surfactants in aqueous solutions and one of the highest in the cement system. The decreasing trend for foam-ability with increasing concentration in the aqueous system is easily explained by the hydrophilic lipophilic balance (HLB), the HLB for this surfactant is very high and it easily forms stable monomers in solution at room temperature. This means that the surfactants potential energy only increases a small amount as it migrates from the interface to the bulk. This low energy barrier promotes easy and fast exchange between the interface and the bulk destabilizing the lamellae.



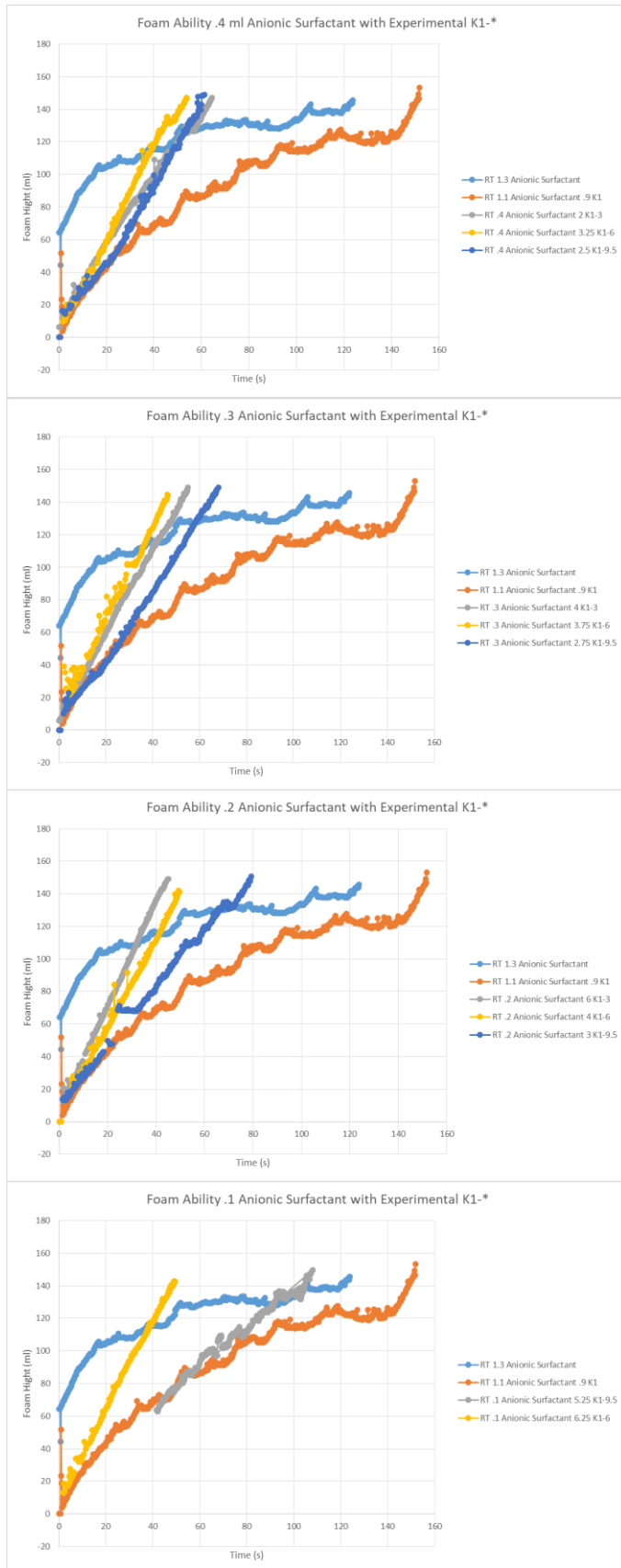


Figure 3: Foam-stability of aqueous Experimental K1-* anionic

surfactant blends found by the Bikerman method.

The foam-stability of a surfactant packages is very important in the creation of foam cement. Therefore, API 10B-4 describes how to test the stability of foam cement systems. Foam-stability is generally described by the BSD or change in BSD over time. So, the foam stability of the surfactant package in a cement system can be found by analyzing the change in BSD within the cement column. The effects of kinetics on the system can be found by comparing the cement columns at different temperatures and constant surfactant loading. Figure 4 shows the preparation of a cement core and the bubble map produced by ImageJ. The white flakes on the pictures to the left are the bubble voids that have been filled in with silica flour, they correspond to the black regions in the pictures to the right. Figure 6 shows a normalized histogram plot of the BSD between these cores shown in Figure 4. There are some very large bubbles present in some of the samples, these bubbles are introduced as the foam cement is poured into the settling tubes and entrains air bubbles from the surroundings. For this reason, we remove bubbles that are outside of the second standard deviation (99.7% inclusive), if this results in more than .3% of the data being removed then data set is kept whole. The BSD inside of the column is extremely uniform and the probability density function shown takes the form of a very narrow Gaussian distribution. The variance in the bottom of the cement core is .0029 mm², .0201 mm² middle bottom, .0051 middle top and .0032 mm² top showing how tightly clustered the BSD truly is. Figure 5 shows all the plots in Figure 4 superimposed upon each other. The distributions show that the BSD is uniform throughout the cement column at room temperature despite the long set time. Figure 7 shows how the bubble size distribution changes as the curing temperature changes. The 70°F and 110°F distributions are essentially the same. If bin .005 and bin .04424 are combined (giving 75% P(x) for RT and 78% P(x) for 111°F) then the two distributions are almost indistinguishable. The 151°F distribution's range dramatically expands to larger bubble size. This is also evidenced in the cement cores; they were a lot more brittle and showed evidence of coalescence and a connected pour network as seen in Figure 5. The general trend found in the cement cores showed that all surfactant packages tested that made a 50% foam quality produced tight uniform BSD in the cement system at room temperature. At 111°F the Experimental K1-3 BSD shifted to the right similarly to Figure 5 and because unstable the Experimental K1-6 and Experimental K1-9.5 remained stable with tight BSD. Somewhere between 111°F and 151°F all surfactant blends started to become unstable, 151°F is close to the decomposition temperature of the anionic surfactant and is also above the cloud point of the Experimental K1-6 and Experimental K1-9.5. This undoubtedly contributed to the greatly increased porosity and coalescence observed within the cores. It must be noted that the packages did initially produce a 50% quality foam and that the cores did hold together and hydrate without shrinkage or settling, however the BSD and hence the mechanical strength of the system is greatly affected.

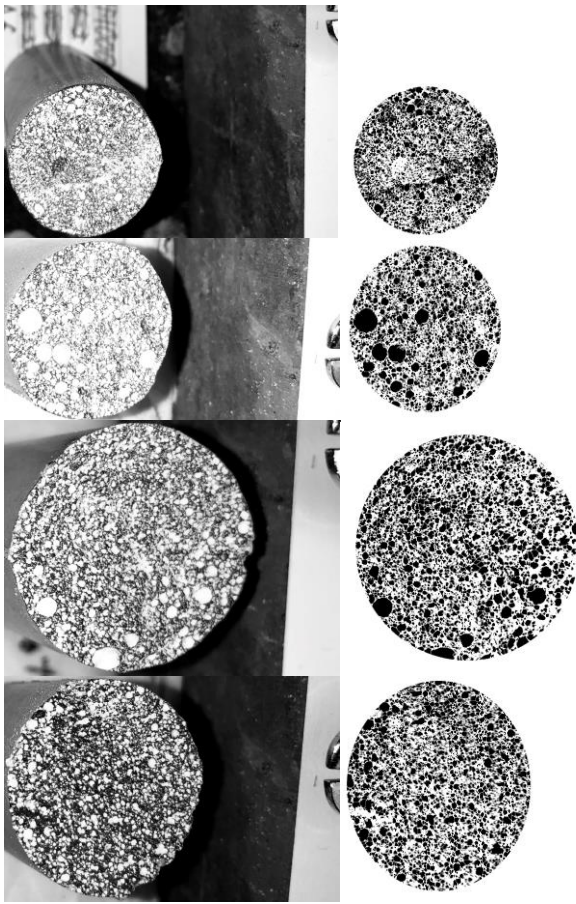


Figure 4: Cured cement cores produced from 1.1ml anionic surfactant and .9ml Experimental K1 at room temperature. From top to bottom the cores are the bottom, middle bottom, middle top and top. The white flakes on the pictures to the left are the bubble voids that have been filled in with silica flour, they correspond to the black regions in the pictures to the right.

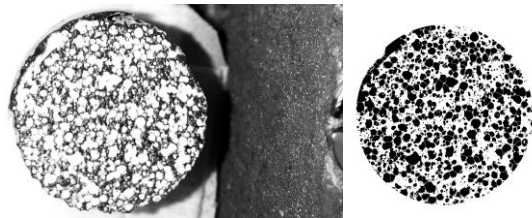
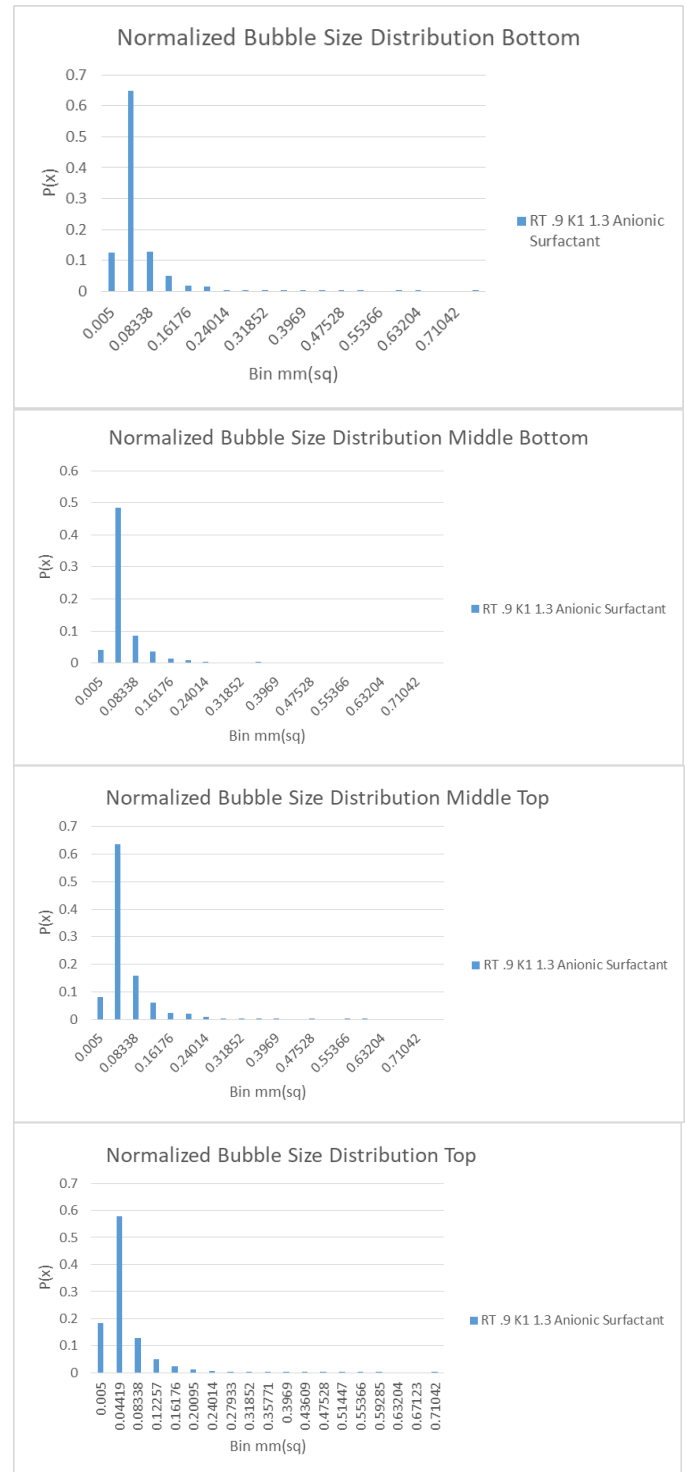


Figure 5: Cured cement core produced from 1.1ml anionic surfactant and .9ml Experimental K1 at 151°F.



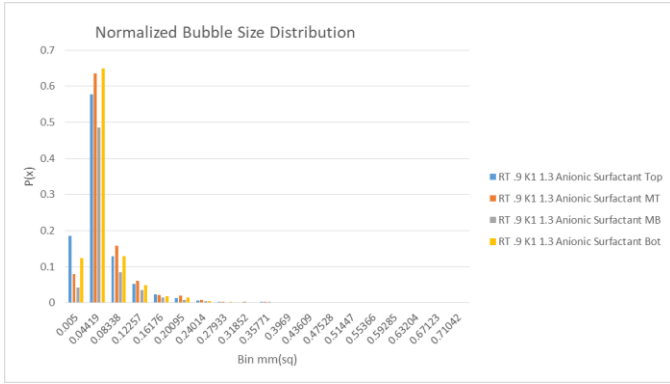


Figure 6: The normalized histogram plot show the BSD for the cement cores shown in Figure 4. The range has been truncated such that 100% of the bubbles are included in the bottom core, 99.7% in the middle bottom core, 99.8% in the middle top core and 100% in the top core.

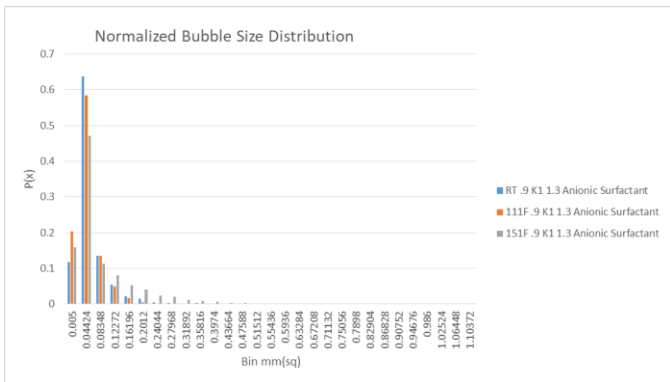
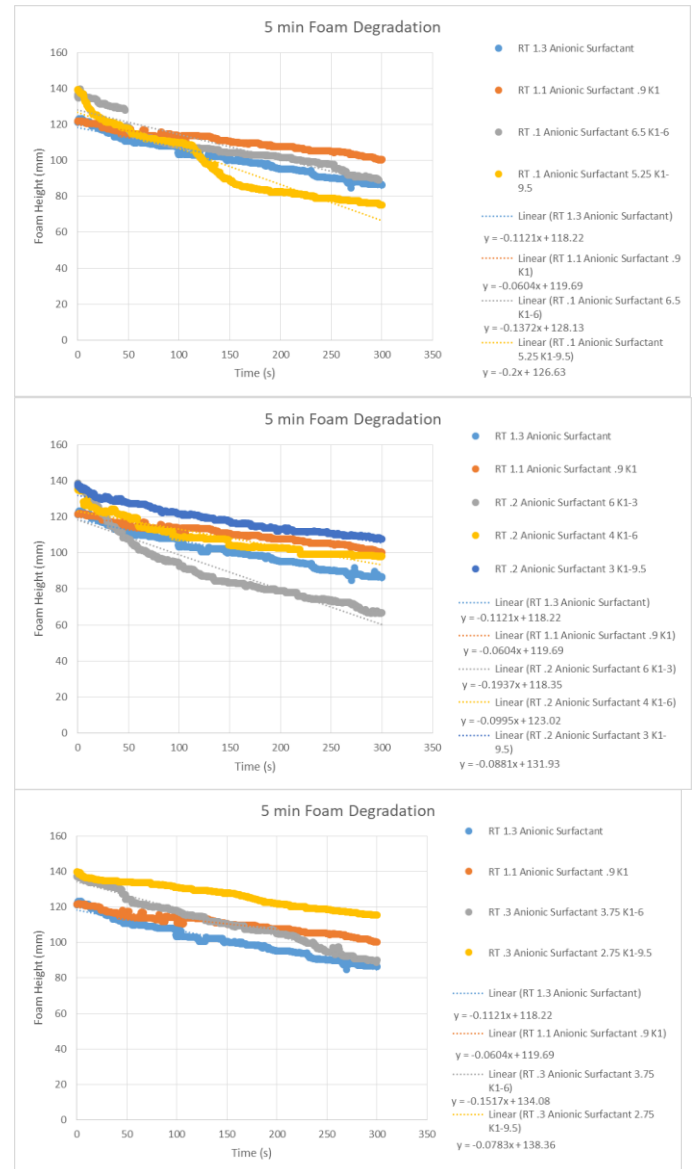


Figure 7: This plot shows a normalized BSD plot for the .9ml Experimental K1 1.3ml anionic surfactant blend at three different temperatures 100% of the data is used and the range is truncated.

The Ross-Miles foam stability test is a standard in industrial applications. It measures the rate of foam degradation within a specified amount of time, here the time intervals presented are 5 minutes and 10 minutes. Figure 8 show the rate of degradation within the first 5 minutes. The anionic surfactant cement foamer created the 4th most stable foam overall. The plots show that the Experimental K1 is the best foam stabilizer tested. Experimental K1 had the smallest slope in 3 out of 5 tests when it was combined with anionic surfactant, Experimental K1-3 was the second-best foam stabilizer with the smallest slope in 2 and second smallest slope in 3 out of 5 plots. This result is consistent with the mechanism for reduction in coulomb repulsion between the anionic head groups eluded to earlier. The Experimental K1 is in fact insoluble in water, the ability of it to interact with the surfactant at the interface, being pulled into solution by the hydrophobe while simultaneously reduce the coulomb repulsion and increasing the strength of the Van der Waals forces makes it the best foam stabilizer. The Experimental K1-3 is highly surface active with an HLB of 11.3. This surfactant will work through the same mechanism as the Experimental K1, the major difference is the size of the head group and the packing parameter at the interface. The Experimental K1 takes up minimal room at the interface and allows more anionic surfactant to pack onto the surface. The

Experimental K1-3 takes up space at the interface, while reducing the coulomb repulsion it doesn't migrate to the interface as quickly as Experimental K1, because of this Experimental K1-3 doesn't stabilize the foam as well. Figure 9 shows the rate of foam degradation after 10 minutes. These plots show that the overall degradation rate converges into two groups. Experimental K1 remains by far the best foam stabilizer. The Experimental K1-3, Experimental K1-6 and Experimental K1-9.5 all had the same general trend in foam degradation after 10 minutes. This is expected as the hydrophobes for these surfactants are the same but have increasing hydrophilicity. This gives different diffusion rates to the interface, so lower hydrophilicity diffuse to the interface faster but approach the same slope overtime as the elasticity of the thin films approach each other.



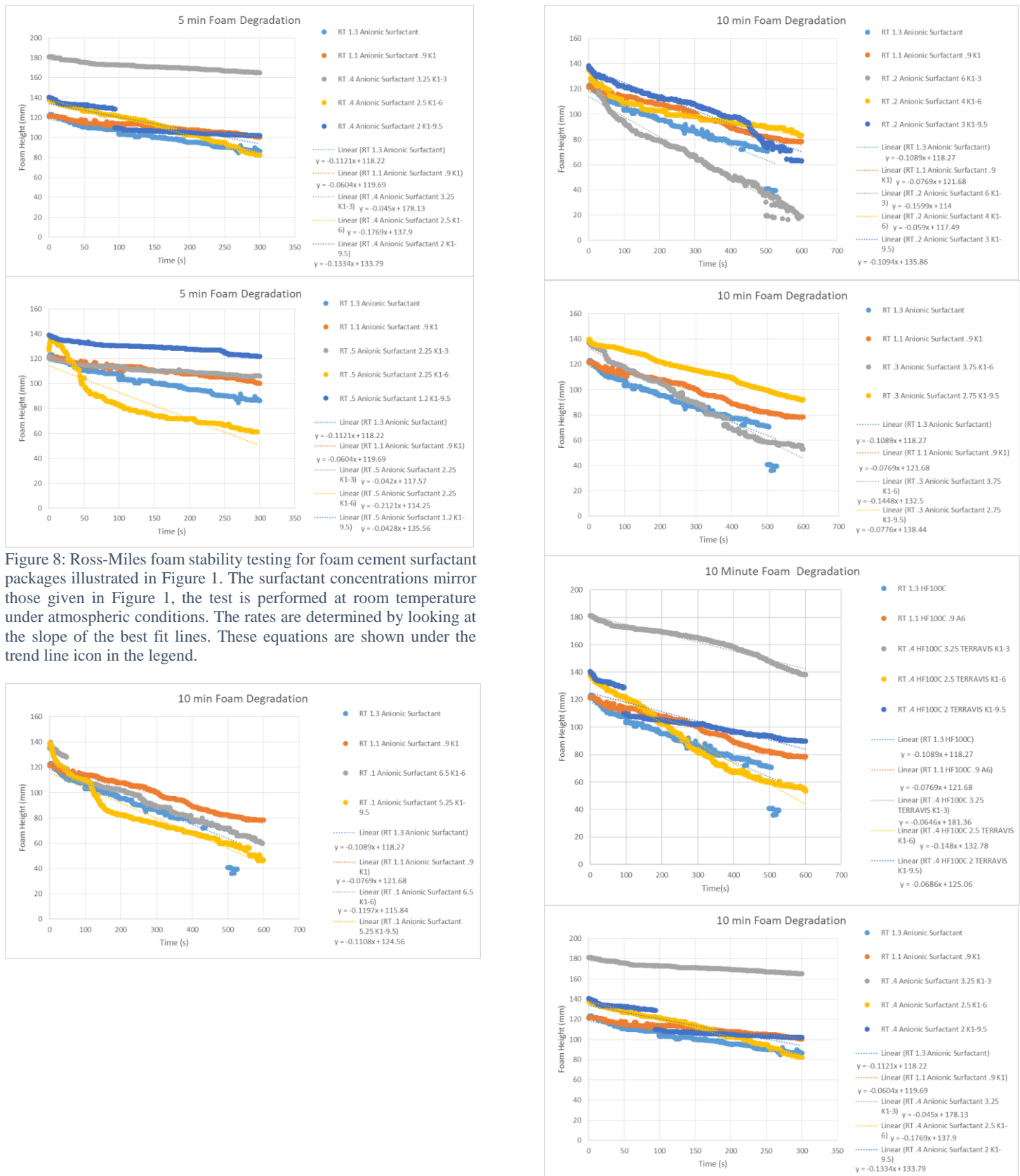


Figure 8: Ross-Miles foam stability testing for foam cement surfactant packages illustrated in Figure 1. The surfactant concentrations mirror those given in Figure 1, the test is performed at room temperature under atmospheric conditions. The rates are determined by looking at the slope of the best fit lines. These equations are shown under the trend line icon in the legend.

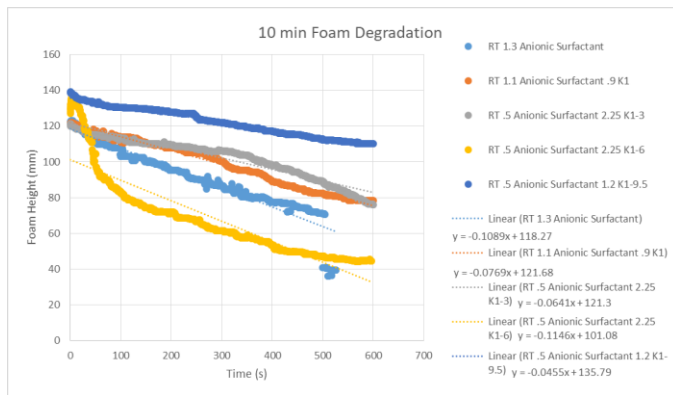


Figure 9: Ross-Miles foam stability testing for foam cement surfactant packages illustrated in Figure 1. The surfactant concentrations mirror those given in Figure 1, the test is performed at room temperature under atmospheric conditions. The rates are determined by looking at the slope of the best fit lines. These equations are shown under the trend line icon in the legend.

Conclusion

The drive to find competitively priced alternatives for chemicals currently used in the oil and gas industry necessitate the introduction of new methods for describing foam-ability and foam-stability. The approach taken in this paper allows for a robust and repeatable methodology for solving this problem. This work shows that industry standard like the Bikerman and Ross-Miles methods work well in aqueous solutions. However, the results don't transfer uniformly to cement systems but can be mitigated through additional development. Many of the packages used in industry are costly and over engineered, allowing low cost alternatives to enter the market.

The results shown for foam-ability and foam-stability are consistent with what is expected from basic surface chemistry models. The effect of adding short chain ethoxylates on the foam-ability is classic, as the surfactant ratios change, they represent the line shape of the bulk phase with an intermediate transition phase when the concentrations are close to 1:1. The foam-stability shown is also expected, the lower HLB surfactants migrate to the interface faster. This decreases the initial foam degradation, however in the long run the bubble stability is governed by the strength of the thin film and the degradation rates converge. The surprising result here is how different the cement system is in both respects. The results presented here show that both aqueous and cement systems should be tested independent of each other, the results of both foam-ability and foam-stability can be vastly different.

This paper presents an approach to enhance an existing anionic foam surfactant cement package. This package is commercially available and used to foam surface and intermediate jobs in shallow wells with low BHST (<140°F). It has been shown that producing blends of this package with other surfactants can enhance the stability and foam-ability. This is important because the anionic surfactant tested in the study is competitively priced to other commercial cement

foamers and readily available. By utilizing the inexpensive Experimental K1-* line of surfactants to enhance the performance of the anionic surfactant you can produce an economically competitive, high performance solution.

Nomenclature

<i>BSD</i>	= Bubble size distribution
<i>HLB</i>	= Hydrophilic lipophilic balance
<i>BHST</i>	= Bottom hole static temperature
<i>CPP</i>	= Critical packing parameter

References

1. Goodwin, K, and Crook. 1992. "Cement Sheath Stress Failure." SPE Drilling Engineering 291-296.
2. Iverson, B, R Darbe, and D McMechan. 2008. "Evaluation of Mechanical Properties of Cements." 42nd US Rock Mechanics Symposium. San Francisco: American Rock Mechanics Association.
3. McElfresh, P, and V Boncan. 1982. "Applications of Foam Cement." Annual Fall Technical Conference and Exhibition of SPE. New Orleans.
4. Peskunowicz, J, and D L Bour. 1987. "FOAM CEMENT SOLVES CEMENTING PROBLEMS IN ALBERTA, CANADA." 38th Annual Technical Meeting of the Petroleum Society of CIM. Calgary: Petroleum Society of CIM. 1459-1470.
5. Prud'homme, R K, and S A Khan. 1996. Foams: Theory, Measurements and Applications. New York: Marcel Dekker.
6. Schneider, C A, W S Rasband, and K W Eliceiri. 2012. "NIH Image to ImageJ: 25 years of image analysis." Nature methods 671-675